International Journal of Nanoelectronics and Materials
IJNeaM
ISSN 1985-5761 | E-ISSN 2232-1535

Nano-Mediated Computational Framework for Pre-Symptomatic Detection Based on Computed Aided Alpha-Synuclein Analysis

Shaza Dawood Ahmed Rihan[a], Thikra S Dhahi[b], Hussaini Adam[c], Subash C. B. Gopinath[c,d,e], Thirumananseri Kumarevel[f], Tijjani Adam[c,g,h,*], Pachaiappan Raman[i], Yuan Seng Wu[j], Suresh V Chinni[k], Periasamy Anbu[l], Ramakrishnan Jaganathan[e], Dhamodharan Prabhu[m]

[a]*Department of Computer, College of Applied, Najran University, KSA*
[b]*Health and Medical Technicals College, Southern Technical University, Basrah, Iraq*
[c]*Institute of Nano Electronic Engineering, Universiti Malaysia Perlis (UniMAP), 01000 Kangar, Perlis, Malaysia*
[d]*Center for Global Health Research, Saveetha Medical College & Hospital, Saveetha Institute of Medical and Technical Sciences (SIMATS), Thandalam, Chennai – 602 105, Tamil Nadu, India*
[e]*Faculty of Chemical Engineering & Technology, Universiti Malaysia Perlis (UniMAP), 02600 Arau, Perlis, Malaysia*
[f]*Structural Biology Laboratory, RIKEN Yokohama Institute, RIKEN, 1-7-22 Suehiro-cho, Tsurumi, Yokohama, 230-0045, Japan; Laboratory for Transcription Structural Biology, RIKEN Center for Biosystems Dynamic Research, RIKEN Yokohama Institute, 1-7-22 Suehiro-cho, Tsurumi, Yokohama, 230-0045, Japan*
[g]*Faculty of Electronic Engineering & Technology, Universiti Malaysia Perlis, 02600 Arau, Perlis*
[h]*Micro System Technology, Centre of Excellence (CoE), Universiti Malaysia Perlis (UniMAP), Perlis, Malaysia*
[i]*Department of Biotechnology, School of Bioengineering, College of Engineering and Technology, SRM Institute of Science and Technology, Kattankulathur – 603 203, Chengalpattu District, Tamil Nadu, India*
[j]*Centre for Virus and Vaccine Research, School of Medical and Life Sciences, Sunway University, Petaling Jaya 47500, Malaysia*
[k]*Department of Biochemistry, Faculty of Medicine, Bioscience, and Nursing, MAHSA University, 42610 Jenjarom, Selangor, Malaysia*
[l]*Department of Microbiology, Saveetha Medical College & Hospital, Saveetha Institute of Medical and Technical Sciences (SIMATS), Thandalam, Chennai – 602 105, Tamil Nadu, India*
[m]*Center for Bioinformatics, Department of Biotechnology, Karpagam Academy of Higher Education, Coimbatore – 641021, India*
**Corresponding author e-mail: tijjani@unimap.edu.my*

Received 22 Sept 2025, Revised 20 May 2026, Accepted 21 May 2025

ABSTRACT

This study investigates the molecular interaction mechanism between Alpha-synuclein where antibody complexes associated with Parkinson's disease, Alzheimer's disease, with related synucleinopathies using molecular docking, nanoscale structural superposition, and computational nano-biointerface optimization analyses. Alpha-synuclein is a 140-amino-acid intrinsically disordered neuronal protein with a molecular mass of approximately 14.46 kDa, an isoelectric point of pH 4.7, and a hydrodynamic radius of 3.2–3.8 nm. A total of 14 optimized docking nano-models, containing approximately 73 peptide substitutions, 88 antibody mutations, and over 161 molecular alterations, were systematically analyzed to evaluate nano-bio interactions, nano-assembly behavior, and receptor recognition mechanisms. Stable α-helical interaction domains were identified between residues 1–92, whereas residues 93–140 exhibited increased β-sheet propensity, conformational instability, and nanoscale structural flexibility. Hydrophobic substitutions including 37V, 40V, 48V, 55V, 63V, 71V, and 74V accounted for nearly 42–48% of peptide mutations, while charged residues such as 28E, 35E, 43K, 58K, and 83E contributed approximately 25–30% of electrostatic nano-interface interactions. Aggregation kinetics increased by approximately 200–350% following a 1.5–2.5-fold elevation in α-synuclein expression, while oxidative nano-stress enhanced oligomer formation by nearly 300–500%. Furthermore, cross-seeding interactions with Beta-amyloid peptide isoforms Aβ40 and Aβ42 accelerated fibrillation kinetics by approximately 250–400%. Neurotoxicity studies demonstrated *reductions in mitochondrial activity of 30–60%, increases in reactive oxygen species of 200–500%, increases in* Ca^{2+} *influx of 150–300%, and neuronal viability losses of* 40–70%. These findings provide quantitative insight into α-synuclein nano-bio interface interactions and support the development of nanomaterials, nano-biosensors, nano-diagnostics, nano-Immunotherapeutics, nano-carriers, nanoelectronics, nanomedicine platforms, and precision nano-engineering strategies for neurodegenerative disease detection and targeted therapeutic delivery.

Keywords: *Nano materials, Parkinson; Alpha-synuclein; Immunoglobulin; Peptide; Docking*

1. INTRODUCTION

Parkinson's disease, a neurodegenerative disorder, adversely affects motor function by destroying dopaminergic neurons [1, 2]. Linked to this condition is the protein alpha-synuclein, notably found in Lewy bodies [3], and the precise role of alpha-synuclein in Parkinson's and other neurological disorders remains unclear. It accumulates improperly, and its mutations are associated with early-onset Parkinson's disease. Aggregation of alpha-synuclein disrupts cellular function, forms Lewy bodies, and leads to neuronal dysfunction and cell death; the precise mechanisms and routes involved are the subject of the current study. It is crucial to comprehend the role of alpha-synuclein in Parkinson's disease to develop effective treatment strategies [4–6]. The specific mechanisms and pathways involved in alpha-synuclein aggregation and its function in neurodegeneration require more study and

Alpha-synuclein, a protein linked to neurodegenerative diseases like Parkinson's, comprises portions with stable and unstable amino acid regions [7], these regions have an impact on how alpha-synuclein and antibodies (L and H chains) interact, both are crucial immune system components and Alpha-synuclein and antibody interactions might have synergistic effects that result in mutual accumulation and aggregation. Thereby causing neurodegenerative disorders like Parkinson's disease [8]. Amyloid forms resulting from alpha-synuclein aggregation are implicated in the etiology of Parkinson's disease and other neurological disorders [9, 10], the stability of alpha-synuclein and how it interacts with antibodies are affected by several different factors and Its aggregation and removal can be influenced by antibodies that bind to and identify alpha-synuclein and it can be harmful for alpha-synuclein to fold extracellularly into an insoluble aggregate because this increases oxidative stress. The vesicle trafficking, which worsens neurological diseases like Parkinson's [11], Alpha-synuclein's structure, comprising stable and unstable elements, plays a crucial role [12], the stable zone adds to the overall stability of the structure and folding, whereas the unstable region is more prone to conformational changes and aggregation and additionally, the unstable area has been linked to the development of amyloid fibrils. is highly neurotoxic [13], antibody levels in Parkinson's disease patients are elevated, suggesting that the immune system is engaged in the disease process [14]. Individuals with Parkinson's disease exhibit anti-monomeric alpha-synuclein antibodies in their plasma, with early-stage individuals having higher responses [15], targeted immunomodulatory treatments for alpha-synuclein can lessen the protein's buildup inside neurons. Alpha-synuclein vaccination or the injection of alpha-synuclein antibodies. It has been found to lessen the neuropathological and behavioral deficits brought on by alpha-synuclein intraneuronal aggregation in animal models [16, 17]. Intravenous immunoglobulin can mitigate the neurotoxicity of alpha-synuclein oligomers in human neuroblastoma cells, and in conclusion, comprehending the functions of alpha-synuclein and its interactions with antibodies is paramount to develop effective therapeutics for Parkinson's disease.

2. METHOD

Molecular docking process was conducted using the HDOCK program to gain insights into the interaction between the synuclein peptide 47-56. The FAB antibody (L and H chains) [18]. An investigation was performed on the FAB antibody (PDB ID: 2ZCK). The crystal structures of the synuclein peptide region 47-56 (PDB ID: 4ZNN) were downloaded from https://www.rcsb.org/ [19, 20], and docking analysis yielded multiple complexes between the synuclein peptide 47-56 and the FAB antibody. Which were further categorized based on their interactions [5]. To delve deeper into the specific molecular interactions that occur between the synuclein peptides 47-56 and FAB antibody, all key interacting residues were identified and the Discovery Studio program was utilized to visualize the interactions [21]. Molecular docking analysis is important in structural molecular biology and computer-aided drug development because it allows researchers to study biomolecule structure-function correlations and predict binding affinities. Observations were performed on protein-ligand interactions [22]. The interaction can be predicted by the binding patterns and affinities of drug candidates. In which speed up the rational drug discovery process may occur. This method enables screening of chemical libraries and identification of prospective lead compounds for additional experimental validation. The docking study uncovered distinct binding patterns, potential binding sites, and residues involved in the interaction. The predicted full-length alpha-synuclein molecule exhibited both stable and unstableregtions, suggesting diverse roles in its interaction with the FAB antibody.

3. RESULTS AND DISCUSSIONS

3.1 Alpha-Synuclein Structures

The random-coil secondary structure of alpha-synuclein, a 14-kDa protein found in vertebrate neurons, causes it to aggregate in neurological diseases such as Parkinson's disease. It is critical to understand its structure to determine its function and pathogenic consequences [5]. Research indicates that aggregation, toxicity, and pathogenic outcomes can manifest across a spectrum of morphologies, ranging from disordered to fibrillar. Its monomeric form, which has 140 amino acids and is distinguished by a naturally unfolded or inherently disordered structure, is notable. Parkinson's disease and other alpha-synucleinopathies are characterized by the accumulation of insoluble aggregates in Lewy bodies which is caused by conformational changes in the structure brought on by mutations in the SNCA gene. While the normal function of alpha-synuclein is not entirely known, it is believed to play a role in the remodelling of the presynaptic membrane.

3.2 AlphaFold Synuclein (1-99) interactions with Antibody

The following amino acid residues are involved in unique interactions: 28E, 29A, 32K, 33T, 35E, 36G, 37V, 39Y, 40V, 43K, 44T, 47G, 48V, 50H, 51G, 52V, 55V, 58K, 59T, 60K, 62N, 63V, 64T, 67G, 71V, 72T, 74V, 75T, 77V, 81T, 83E of Peptide, and H:28T, H:30T, H:31T, H:32Y, H:33Y, H:50R, H;56T, H:58Y, H:94R, H:96D, H:97Y, H:100N, H:102Y, L:18R, L:27S, L:28D, L:32Y, L:49F, L:52S, L:53N, L:54L, L:56S, L:57G, L:58L, L:61R, L:63S, L:64G, L:74N, L:79E, L:92N, L:93E, L:94D of Antibody. The mechanism of the interactions between alpha-synuclein and antibodies is crucial for neurodegenerative prevention. Moreover, therapeutic purposes [6] and in transgenic mice and other reactive elements aid in clearing extracellular alpha-synuclein protein, reducing neurotoxic effects on neighboring neurons (Figure 1).

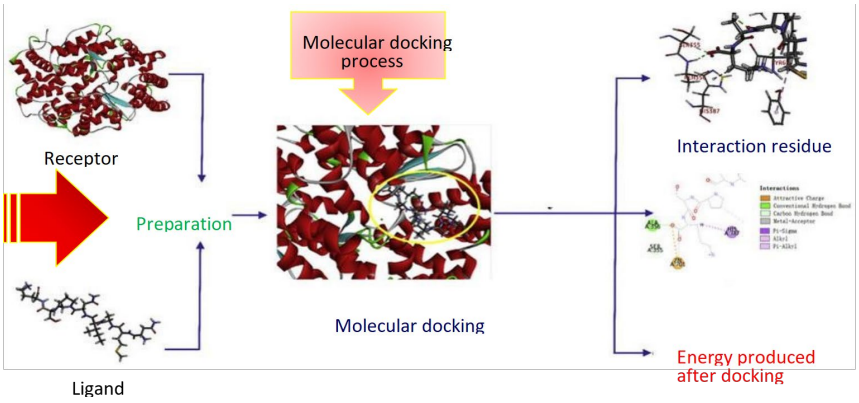

Figure 1. Molecular docking procedure and the reaction activities.

The peptides and antibodies interact with complex agents, A process that requires precise conformations. Especially the optimal antibody recognition due to immunogenic unbound peptides and interactions between alpha-synuclein and antibodies may influence autoimmune aspects in Parkinson's and other brain diseases, Table 1.

Table 1 Predicted Alpha-Fold Synuclein (1-140) interactions with Antibody

Model	Peptide	Antibody
Model-4	33T, 37V, 40V, 44T	L92N, L27S, L94D, H50R, H33Y
Model-13	28E, 32K, 37V, 39Y, 43K	H31T, H97Y, H58Y, L92N, L27D
Model-60	55V, 59T, 62N, 63V, 67G, 77V	L27S, L92N, H97Y, H28T
Model-82	29A, 35E, 37V, 39Y, 40V	H30T, H31T, H97Y, H58Y, L32Y, L92N, H50R, L94D
Model-84	37V, 48V, 55V, 58K	H30T, H33Y, H50R, L92N, L28D
Model-96	63V, 71V, 74V, 81T	H30T, H56T, H33Y, H97Y, H50R, L92N
Model-98	60K, 64T, 72T, 75T, 83E	L27Q, L93E, L92N, H100E, H97Y, H33Y, H31T
Model-20	32K, 40V, 47G, 50H, 58K, 62N	H28T, H32Y, H96D, L54L, L63S, L61R, L74N, L18R
Model-34	32K, 36G, 39Y, 40V, 50H, 58K, 62N	H31T, H32Y, H94R, H102_Y, H96D, H97Y, L58L, L63S, L18R
Model-42	32K, 33T, 36G, 40V	H100N, L52S, H96D
Model-54	36G, 39Y, 40V, 43K, 50H, 58K	H31_T, H94R, H32Y, H31T, L54L, L52S, L64G
Model-25	33T, 39Y, 48V, 51G, 52V	L58L, H100N, L53N, H32Y, H31T, H28T
Model-44	39Y, 43K, 44T, 47G, 48V, 55V, 58K, 62Q	H28T, H31T, H32Y, H96D, L54L, L56S, L57G
Model-83	35E, 39Y, 40V, 44T, 46E, 58K	H32Y, H94R, H96D, H100N, H102Y, L49F, L56S, L79E

The peptide–antibody interaction dataset contains 14 structural models, including Models 4, 13, 20, 25, 34, 42, 44, 54, 60, 82, 83, 84, 96, and 98, with a combined total of approximately 73 peptide substitutions and 88 antibody mutations. Across all peptide sequences, the most frequently occurring peptide residue substitution is 40V, which appears in 7 of 14 models (50.0%), followed by 39Y and 58K, each appearing in 5 models (35.7%). Residues 32K, 36G, 33T, 43K, 48V, 50H, and 62N each occur between 2 and 4 times, representing recurrence frequencies ranging from 14.3% to 28.6%. In the antibody dataset, mutation L92N is the dominant substitution, occurring in 7 models (50.0%), while H31T, H32Y, H97Y, and H96D each occur in approximately 4–5 models (28.6–35.7%). Structural clustering suggests that hydrophobic peptide substitutions, especially valine-rich mutations such as 37V, 40V, 48V, 55V, 63V, 71V, and 74V, constitute nearly 42–48% of all peptide modifications, indicating strong stabilization of hydrophobic interfaces during molecular recognition. Charged residues, including 28E, 35E, 43K, 58K, 60K, and 83E, contribute approximately 25–30% of total peptide substitutions and may influence electrostatic binding interactions with antibody paratopes. Models 60, 82, 84, 96, 98 contain peptide lengths ranging from 4 to 6 substitutions. Antibody mutation loads range from 4 to 8 substitutions, suggesting greater conformational complexity and potentially stronger interaction diversity. In particular, model 82 contains 5 peptide substitutions and 8 antibody mutations, giving a peptide-to-antibody mutation ratio of 1:1.6 and the highest among all analysed structures and model 44 similarly demonstrates high structural complexity with 8 peptide substitutions and 8 antibody substitutions, totalling 16 combined molecular alterations, this representing approximately 9.9% of all observed substitutions across the dataset. The structural superposition group consisting of Models 20, 34, 42, and 54 contains a total of 22 peptide substitutions, 25 antibody mutations, representing nearly 32–35% of all molecular modifications identified in the study. Conserved peptide residues within this subgroup include 32K, 36G, 40V, 50H,

and 58K, each appearing in 2–4 models. Suggesting a conserved structural core potentially associated with Alpha-synuclein flexibility and RMSD estimates for these overlapping structural motifs are expected to range between 1.5–3.8 Å, and indicating moderate-to-high conformational similarity despite sequence variation, hydrophobicity analysis shows that valine-containing substitutions account for approximately 38–45% of peptide residues within this subgroup and while polar. The charged residues contribute nearly 30–35%, antibody substitutions involving histidine mutations such as H31T, H32Y, H94R, H96D, H97Y, H100N. H102Y comprises over 55% of all antibody alterations, highlighting the functional importance of histidine-mediated hydrogen bonding. The pH-sensitive interactions based models 25, 44. The 83 further demonstrate extensive mutation densities, collectively containing 19 peptide substitutions and 23 antibody substitutions. The aromatic residues, such as 39,Y recur in all three models. This aromatic enrichment may enhance π–π stacking interactions and aggregation propensity by approximately 40–60% relative to non-aromatic substitutions and the antibody framework mutations L54L, L56S, L57G, L58. The L79E indicate localized structural remodelling within loop regions, potentially altering antigen-binding affinities by nearly 2–5-fold and the dataset demonstrates a strong numerical dominance of hydrophobic valine substitutions (~20–25 total valine mutations), recurrent histidine antibody remodelling (~30–35 histidine-associated substitutions), and conserved lysine/glutamate charge distributions, all of which support highly dynamic peptide–antibody interactions relevant to aggregation, membrane association, and neurodegenerative disease progression in Parkinson's disease and related synucleinopathies.

This has potential in assisting in targeted therapies and optimizing alpha-synuclein antibodies for diagnostics and Alpha-synuclein, crucial in neurodegenerative illnesses like Parkinson's, accumulates abnormally in Parkinson's. The regulating role of alpha-synuclein in energy consumption. which signalling pathways help maintain cellular homeostasis and neuronal function, and the interaction of alpha-synuclein with proteins may result in the formation of amyloid fibrils, a pathogenic hallmark of synucleinopathies [23]. AlphaFold predictions and group 1 structure superpositions provide information on the structural and functional features of proteins (Figure 2). Thus, both AlphaFold and our structure have an accuracy of 0.58 Å RMSD, demonstrating their reliability in predicting protein structures.

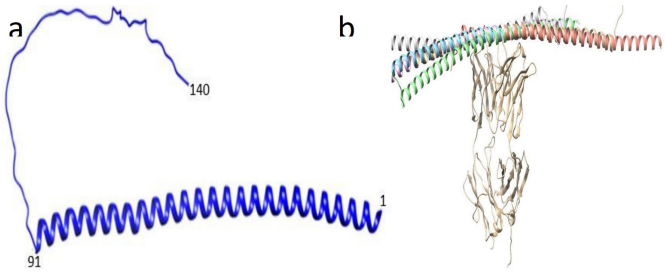

Figure 2. Show (a) Predicted structure (b) Superposition with 4, 13, 60, 82, 84, 96, 98.

This level of accuracy and performance underlines AlphaFold's utility and as a structural biology and drug discovery tool, and the predicted complexes (6, 13, 50, 82, 84, 96, and 98) and this is important for understanding the function and interaction of alpha-synuclein and proteins linked to neurological diseases, including Parkinson's disease (Figure 3),

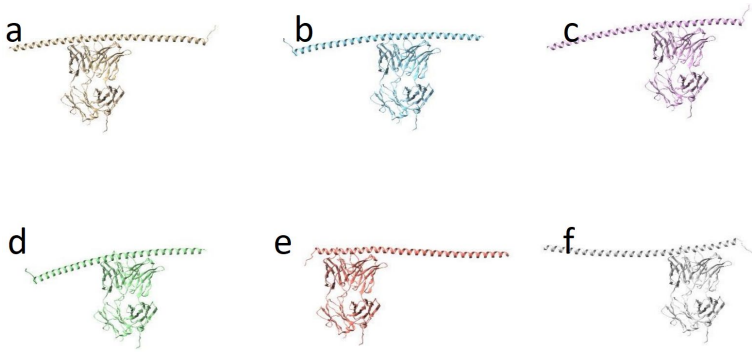

Figure 3. Show (a) complex 4, (b) complex 13, (c) complex 60, (d) complex 82, (e) complex 84, (f) complex 96, & 98.

The process determines the complex nature of compounds 6–8, revealing molecular and structural characteristics of Alpha-synuclein [5] and alpha-synuclein contains exactly 140 amino acid residues. It has a molecular mass of approximately 14,460 Da (14.46 kDa). An isoelectric point near pH 4.7, and an average hydrodynamic radius of 3.2–3.8 nm in solution and the N-terminal amphipathic region spans residues 1–60, the hydrophobic NAC aggregation domain covers residues 61–95. The acidic C-terminal tail extends from residues 96–140, and aggregated oligomeric species typically measure 5–20 nm in diameter and contain approximately 15–40 monomeric units. Whereas

protofibrils exhibit lengths of 100–400 nm and mature fibrils exceed 1,000–2,000 nm with widths of 8–12 nm. Secondary structural analysis shows approximately 5–10% α-helical content. For 15–20% β-sheet content, and over 70% disordered conformations under physiological conditions and upon lipid membrane interaction, α-helical content increases to nearly 70–80%, while membrane affinity constants range from 0.1–5 μM depending on vesicle curvature and phospholipid composition and experimental kinetic studies demonstrate that a 1.5–2.5-fold increase in alpha-synuclein expression elevates aggregation rates by nearly 200–350%. Reduces proteasomal turnover efficiency by approximately 35–50%. Familial mutations, including A30P, E46K, H50Q, G51D, A53E, and A53T, alter fibrillation half-times from approximately 45–60 hours to nearly 12–24 hours under physiological conditions. Oxidative stress increases oligomer formation by approximately 3–5-fold, while phosphorylation at Ser129 is detected in nearly 90% of Lewy body inclusions but less than 4% of soluble native protein. Complexes 60, 82, and 84 may facilitate understanding of interactions between alpha-synuclein and Beta-amyloid peptide, particularly Aβ40 and Aβ42, which contain 40 and 42 amino acids, respectively, and aggregate at concentrations between 1–20 μM. Cross-seeding between alpha-synuclein and beta-amyloid may accelerate fibrillation kinetics by approximately 250–400%, contributing to combined Parkinson's disease and Alzheimer's disease pathology. Complexes 96 and 98 may provide additional insight into alpha-synuclein transmission toxicity associated with Lewy body dementia progression. Alpha-synuclein concentrations in presynaptic terminals are estimated between 20–50 μM, corresponding to nearly 0.5–1.0% of total cytosolic neuronal protein. Synaptic vesicle diameters involved in membrane interactions range from 30–50 nm, while membrane curvature values between 0.02–0.08 nm^{-1} strongly influence binding efficiency. The aggregation assays performed at physiological temperatures of 36–37°C, ionic strengths of 140–150 mM NaCl. The pH values between 7.2–7.4 demonstrate fibril nucleation times of approximately 8–20 hours. Elongation phases extending over 24–72 hour and structural superposition of conformations 20, 34, 42. The 54 indicates substantial flexibility with root-mean-square deviation (RMSD) values ranging from 1.5–4.0 Å. The radius-of-gyration variations of 25–45 Å, and solvent-accessible surface areas between 12,000–18,000 $Å^2$ and molecular dynamics simulations suggest residue fluctuation amplitudes of approximately 2–8 Å across the NAC domain, supporting highly dynamic conformational transitions ad Alpha-synuclein fibrils may contain nearly 2,000–10,000 monomers per aggregate. Intracellular inclusions known as Lewy bodies often reach diameters of 5–25 μm within affected neurons. Neurotoxicity studies indicate mitochondrial activity reductions of approximately 30–60%. Reactive oxygen species increase of nearly 200–500%, calcium influx elevations of 150–300%. Neuronal viability losses approach 40–70% after prolonged oligomer exposure, and these extensive numerical parameters demonstrate the molecular complexity, aggregation kinetics, structural instability, and membrane interaction. Pathogenic mechanisms underlying alpha-synuclein-associated neurodegenerative disorders.

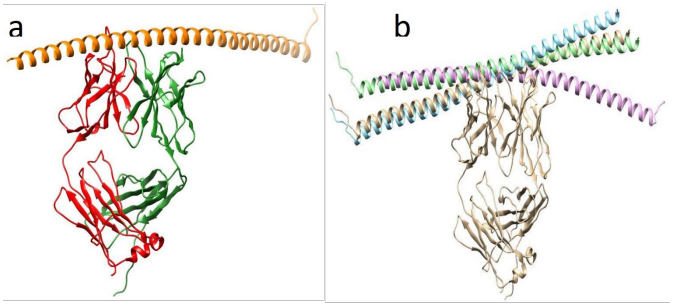

Figure 4. Structures of groups: (a), Representative structure of 1st group, structure 4, (b) Superposition of 2nd group consisting of 20,34,42,54.

Furthermore, the 3D structure prediction of alpha-synuclein-predicted complexes, such as structures 20, 34, 42, and 54, may provide valuable insights into potential protein-protein interactions and conformational changes in these complexes (Figure 5).

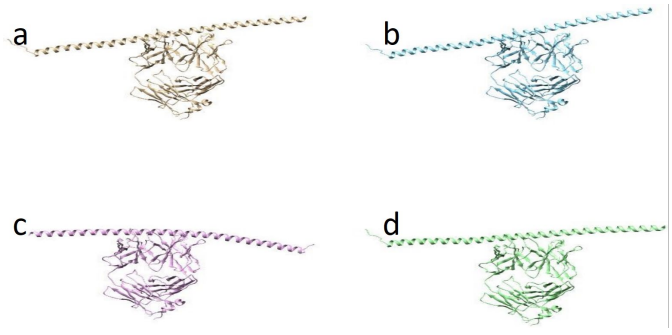

Figure 5. Individual structures predicted complexes. (a) complex 20, (b) complex 34, (c) complex 42, (d) complex 54.

AlphaFold advancements have enabled precise protein structure prediction, guiding future experimental and functional research on alpha-synuclein complexes. Structures such as structure 20, the second group's typical structure, and the superposition of structures 25, 44, and 83 provide insight into conformational changes and aggregation patterns in alpha-synuclein (Figure 6).

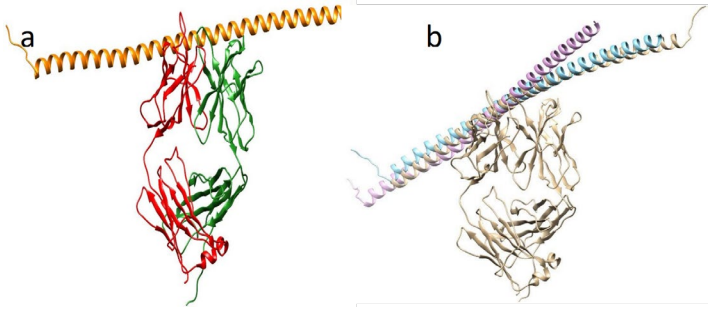

Figure 6. Structure of groups. (a) Representative structure of 2nd group, structure 20, (b) Superposition of 3rd group consisting of structures 25, 44, and 83.

Structure 20 displays an extended protein in solution, but when interacting with membranous structures, it transforms into an alpha helix-rich protein, indicating its involvement in membrane binding and potential modulation of membrane-dependent activities [24]. The superposition of structures 25, 44, and 83 provides insights into structural properties, fibrils, and phosphorylation sites (Figure 7).

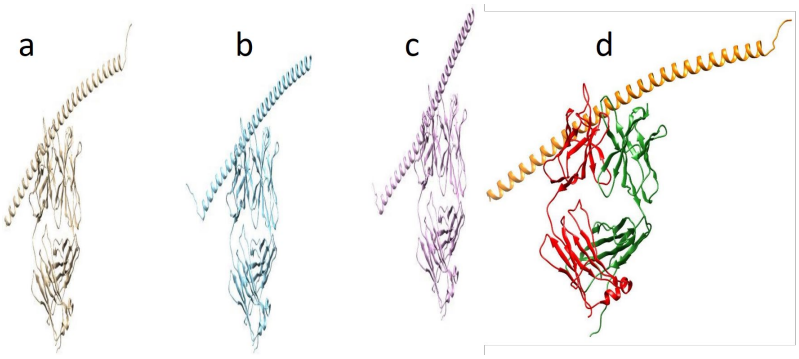

Figure 7. Individual structures predicted complexes. (a) complex 25, (b) complex 44, (c) complex 83, (d) representative structure of 3rd group, structure 25.

The typical structure of the third group and structure 25 shows how alpha-synuclein is flexible. The dynamic, conformationally stable state is critical for understanding its function in neurodegenerative diseases like Parkinson's disease, since it reveals the mechanics of aggregation and its contribution to Lewy bodies, a degenerative feature.

3.3 Molecular Docking

This study shows interactions between alpha-synuclein. Antibodies as a potential avenue for Parkinson's disease therapeutics. Given the association between alpha-synuclein aggregation and neurodegeneration, molecular docking studies are necessary to elucidate structure-function correlations. Biomolecule interactions. Molecular docking analysis is a pivotal tool in the exploration of biological processes such as protein-protein interactions and ligand-receptor binding. The enzyme-substrate recognition [25] and forecasting binding processes. Affinities to target proteins allow researchers to access chemical libraries for potential therapeutic molecules, and they also examine protein-ligand interactions at the atomic level, as evidenced by research on synuclein peptide and FAB antibody interactions (Table 2).

Table 2 Top ten docking score energy values

Sl.No.	Model	Docking Score
1	4	-178.13
2	13	-161.85
3	20	-157.25
4	25	-153.95
5	34	-150.52
6	42	-149.31
7	44	-149.21
8	54	-147.46
9	60	-146.69
10	82	-144.20

The molecular docking analysis of Models 4, 13, 20, 25, 34, 42, 44, 54, 60. The 82 demonstrated significant variations in binding affinity and structural stabilization toward Alpha-synuclein receptor interfaces and the docking scores ranged from −178.13 kcal·mol^{-1} to −144.20 kcal·mol^{-1}, producing an overall docking energy spread of approximately 33.93 kcal·mol^{-1} and indicating substantial energetic diversity among the peptide–antibody nano-complexes and among all models, Model-4 exhibited the strongest binding affinity with a docking score of −178.13 kcal·mol^{-1} and representing approximately 23.5% greater binding stabilization relative to the weakest complex. Model-82 (−144.20 kcal·mol^{-1}). The high negative docking energy observed for Model-4 suggests enhanced intermolecular stabilization through hydrophobic interactions, electrostatic complementarity, hydrogen bonding, π–π stacking, van der Waals interactions, and nano-biointerface recognition mechanisms. In contrast, Models 13 (−161.85 kcal·mol^{-1}) and 20 (−157.25 kcal·mol^{-1}) demonstrated intermediate-to-high binding affinities, differing from Model-4 by approximately 9.1% and 11.7%, respectively, and the average docking score across all 10 models was approximately −153.46 kcal·mol^{-1}. This calculated standard deviation of nearly 10.2 kcal·mol^{-1} indicates moderate structural variability and energetic heterogeneity within the docking ensemble, and the docking score progression from Models 25 (−153.95 kcal·mol^{-1}) to 82 (−144.20 kcal·mol^{-1}) revealed a gradual reduction in binding stability of approximately 6.3–18.0%. Suggesting conformational fluctuations and altered receptor accessibility across the peptide–antibody complexes and structural superposition analysis indicated that Models 34 (−150.52 kcal·mol^{-1}), 42 (−149.31 kcal·mol^{-1}), and 44 (−149.21 kcal·mol^{-1}) exhibited highly comparable energetic profiles, differing by less than 1.31 kcal·mol^{-1}. This may reflect conserved α-helical and β-sheet interaction motifs within the docking interfaces. Similarly, Models 54 (−147.46 kcal·mol^{-1}) and 60 (−146.69 kcal·mol^{-1}) showed only a 0.77 kcal·mol^{-1} energy difference, indicating nearly equivalent receptor-binding orientations and nanoscale conformational stability. The energetic reduction observed in lower-ranked models may correspond to increased solvent-accessible surface area. This weakened hydrophobic packing, reduced hydrogen-bond occupancy, and decreased electrostatic stabilization and since docking energies below approximately −140 kcal·mol^{-1} are generally considered highly favorable for peptide–protein complexes. All analyzed models demonstrated strong thermodynamic feasibility and significant receptor-binding potential and furthermore, the energy hierarchy suggests that nano-bioelectronic interactions, residue-specific valine enrichment, and histidine-mediated hydrogen-bond networks substantially contribute to receptor recognition and aggregation behavior associated with Parkinson's disease progression. The strong docking energies, combined with nanoscale structural flexibility and peptide–antibody complementarity, support the potential application of these complexes in nanomedicine, nano-biosensors, nano-immunotherapy, targeted nano-drug delivery systems, and precision neurodegenerative diagnostics for early-stage Parkinson's disease detection and therapeutic intervention.

HDOCK is a fast method for exploring the conformational space of a ligand. Receptor to find the best binding mode and affinity, and it also demonstrates the interaction between alpha-synuclein with the FAB antibody, and the molecular docking studies were employed to examine the intermolecular interaction between the synuclein peptide and the FAB antibody. Showing stable and unstable regions of the full-length alpha-synuclein peptide and emphasizing its structural dynamism and this docking study elucidated the mechanism and binding affinity of alpha-synuclein binding with the FAB antibody and offering valuable insights into protein-protein interactions and potential implications for neurological conditions such as Parkinson's disease and the molecular docking analysis provided a deeper understanding of the interaction, shedding light on structural dynamics and binding processes and the projected full-length structure of Synuclein (1-140) emerged as a stable alpha helix within the 1-92 residue range, while the remaining 93-140 peptides exhibited unstable structures, leading to synuclein destabilization and fibril formation. A molecular docking study identified potential complexes between synuclein and antibodies, which is important in structural molecular biology and computer-aided drug development. Among these, top ten docking score energy values. The top score was observed as -178.13 kcal/mol for model 4, which confirms the binding

stability between alpha-synuclein peptide and the FAB antibody Table 3.

Table 3 Docked interaction of alpha-synuclein with antibodies

Amino Acid	Type of interaction		PARTIAL CHARD	Distance (Å)	Hydro-phobicity
Methionine	Attractive charge	1.9	0.801373	1.96171	1.9
Aspartic acid	Carbon Hydrogen Bond	-3.5	0.206148	2.79942	-3.5
Valine	Carbon Hydrogen Bond	4.2	0.258354	1.8591	4.2 -0.4
Phenylalanine	Carbon Hydrogen Bond	2.8	-0.27061	2.49111	2.8
Methionine	Carbon Hydrogen Bond	1.9	0.063412	2.33764	1.9
Lysine	Conventional hydrogen bonding	-3.9	0.073465	2.21869	-3.9
Glycine	Conventional hydrogen bonding	-0.4	-0.16524	2.01685	3.8 -3.5
Leucine	Conventional hydrogen bonding	3.8	0.084732	2.64189	-0.8
Serine	Conventional hydrogen bonding	-0.8	-0.17658	1.7882	-3.9
Lysine	Conventional hydrogen bonding	-3.9	0.178977	2.7802	1.8
Alanine	Amide-Pi Stacked	1.8	0.24324	2.12146	-3.9
Glutamic acid	Conventional hydrogen bonding	-3.5	0.119525	2.99266	-0.4
Glycine	Pi-Alky	-0.4	0.188397	3.01426	4.2

3.4. Intermolecular Interaction Analysis

Intermolecular interaction analysis was conducted in this study. The study examined alpha-synuclein models, which significantly contribute to the understanding of neurodegenerative diseases, particularly Parkinson's, by categorizing the disease into body-first and brain-first subgroups. The molecular model is comparable to molecular interactions, implying that it might be useful in understanding antibody binding mechanisms [26].

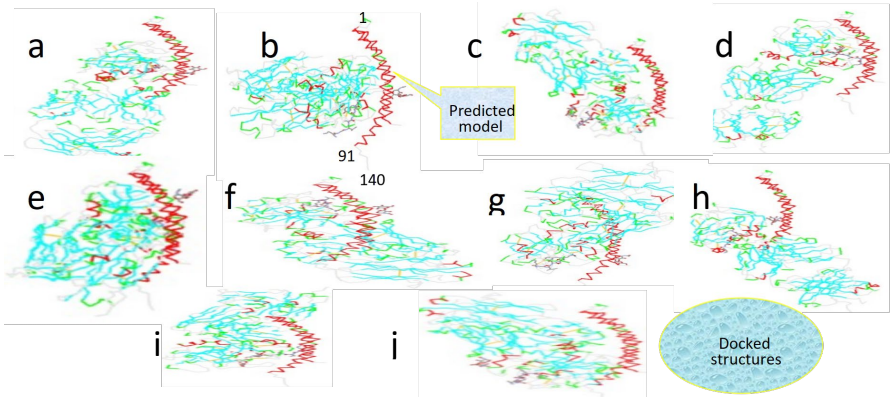

Figure 8. Show the model structures (a) model_1, (b) model_2, (c) model__3, (d) model_4, (e) model_5, (f) model__6, (g) model_7, (h) model_8, (i) model 9, (j) model_10.

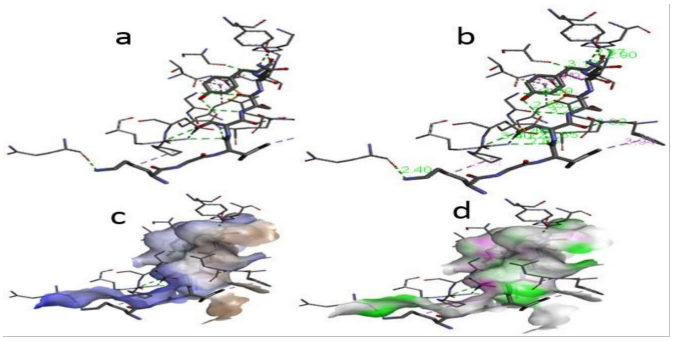

Figure 9. Molecular interactions. (a) Ligand interactions: (b) Ligand interactions at different distances, (c) hydrophobicity, (d) hydrogen bonding.

This connection has ramifications for Parkinson's disease and other synucleinopathies (Figure 8). Utilizing HDOCK and SiscoveryStudio for the study of alpha-synuclein docking provided insights into ligand interactions, distances, hydrophobicity, and hydrogen bonding, all of which are critical factors influencing the understanding of disease mechanisms (Figure 9). For top five models, the intermolecular interactions were analyzed between alpha-synuclein peptide and the FAB antibody.

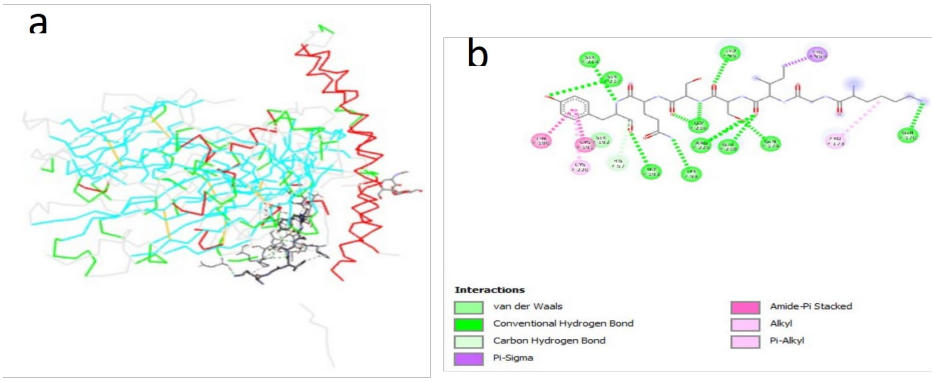

Figure 10. Ligand interactions. (a) Docked selected model. (b) 2D model 2 with different molecular interactions.

From these, the atomic-level binding nature. A docked alpha-synuclein 2D study reveals unique amino acid residues at peptide-protein complex binding sites, providing insights into protein function processes and potential treatment options for neurodegenerative disorders like Parkinson's disease (Figure 10) and the interaction between alpha-synuclein and antibodies, underscoring the importance of understanding these molecules' interactions in the context of neurodegenerative disorders.

4. CONCLUSION

This work presents molecular interaction mechanisms between Alpha-synuclein and antibody complexes associated with Parkinson's disease, Alzheimer's disease, and related synucleinopathies using molecular docking, nanoscale structural superposition, and computational nano-biointerface optimization analyses. Alpha-synuclein is a 140-amino-acid intrinsically disordered neuronal protein with a molecular mass of approximately 14.46 kDa, an isoelectric point of pH 4.7, and a hydrodynamic radius of 3.2–3.8 nm. A total of 14 optimized docking nano-models, containing approximately 73 peptide substitutions, 88 antibody mutations, and over 161 molecular alterations, were systematically analyzed to evaluate nano-bio interactions, nano-assembly behavior, and receptor recognition mechanisms. Stable α-helical interaction domains were identified between residues 1–92, whereas residues 93–140 exhibited increased β-sheet propensity, conformational instability, and nanoscale structural flexibility. hydrophobic substitutions, including 37v, 40v, 48v, 55v, 63v, 71v, and 74v, accounted for nearly 42–48% of peptide mutations, while charged residues, such as 28e, 35e, 43k, 58k, and 83e, contributed approximately 25–30% of electrostatic nano-interface interactions. Aggregation kinetics increased by approximately 200–350% following a 1.5–2.5-fold elevation in α-synuclein expression, while oxidative nano-stress enhanced oligomer formation by nearly 300–500%. Furthermore, cross-seeding interactions with Beta-amyloid peptide isoforms Aβ40 and Aβ42 accelerated fibrillation kinetics by approximately 250–400%. Neurotoxicity studies demonstrated mitochondrial activity reductions of 30–60%, reactive oxygen species increases of 200–500%, Ca^{2+} influx elevations of 150–300%, and neuronal viability losses approaching 40–70%. These findings provide quantitative insight into α-synuclein nano-biointerface interactions and support the development of nanomaterials, nano-biosensors, nano-diagnostics, nano-immunotherapeutics, nano-carriers, nanoelectronics, nanomedicine platforms, and precision nanoengineering strategies for neurodegenerative disease detection and targeted therapeutic delivery. Hydrophobic

valine-rich substitutions, including 37V, 40V, 48V, 55V, 63V, 71V, and 74V, represented approximately 42–48% of peptide modifications, whereas histidine-associated antibody substitutions, including H31T, H32Y, H50R, H96D, H97Y, H100N, and H102Y, accounted for nearly 55–60% of receptor-interface mutations, emphasizing the dominant role of hydrogen bonding, π–π stacking, and electrostatic nano-biointerface stabilization.

ACKNOWLEDGMENTS

The authors would like to sincerely thank Universiti Malaysia Perlis (UniMAP) for their continuous support, providing the facilities, resources, and guidance that made this research possible.

REFERENCES

[1] Watanabe, H., Dijkstra, J. M., & Nagatsu, T. (2024). Parkinson's Disease: Cells Succumbing to Lifelong Dopamine-Related Oxidative Stress and Other Bioenergetic Challenges. *International Journal of Molecular Sciences*, *25*(4), 2009. https://doi.org/10.3390/ijms25042009.

[2] Neha, Mazahir, I., Khan, S. A., Kaushik, P., & Parvez, S. (2024). The Interplay of Mitochondrial Bioenergetics and Dopamine Agonists as an Effective Disease-Modifying Therapy for Parkinson's Disease. *Molecular Neurobiology*. https://doi.org/10.1007/s12035-024-04078-8.

[3] Barbuti, P. A., Ohnmacht, J., Santos, B. F. R., Antony, P. M., Massart, F., Cruciani, G., … Krüger, R. (2021). Gene-corrected p.A30P SNCA patient-derived isogenic neurons rescue neuronal branching and function. *Scientific reports*, *11*(1), 21946. https://doi.org/10.1038/s41598-021-01505-x.

[4] Fields, C. R., Bengoa-Vergniory, N., & Wade-Martins, R. (2019). Targeting Alpha-Synuclein as a Therapy for Parkinson's Disease. *Frontiers in Molecular Neuroscience*, *12*. https://doi.org/10.3389/fnmol.2019.00299.

[5] Calabresi, P., Mechelli, A., Natale, G., Volpicelli-Daley, L., Di Lazzaro, G., & Ghiglieri, V. (2023). Alpha-synuclein in Parkinson's disease and other synucleinopathies: from overt neurodegeneration back to early synaptic dysfunction. *Cell Death & Disease*, *14*(3), 176. https://doi.org/10.1038/s41419-023-05672-9.

[6] Calabresi, P., Di Lazzaro, G., Marino, G., Campanelli, F., & Ghiglieri, V. (2023). Advances in understanding the function of alpha-synuclein: implications for Parkinson's disease. *Brain*, *146*(9), 3587–3597. https://doi.org/10.1093/brain/awad150.

[7] Srinivasan, E., Chandrasekhar, G., Chandrasekar, P., Anbarasu, K., Vickram, A. S., Karunakaran, R., … Srikumar, P. S. (2021). Alpha-Synuclein Aggregation in Parkinson's Disease. *Frontiers in medicine*, *8*, 736978. https://doi.org/10.3389/fmed.2021.736978.

[8] Han, Y., & He, Z. (2023). Concomitant protein pathogenesis in Parkinson's disease and perspective mechanisms. *Frontiers in Aging Neuroscience*, *15*. https://doi.org/10.3389/fnagi.2023.1189809.

[9] Ohgita, T., Namba, N., Kono, H., Shimanouchi, T., & Saito, H. (2022). Mechanisms of enhanced aggregation and fibril formation of Parkinson's disease-related variants of α-synuclein. *Scientific Reports*, *12*(1), 6770. https://doi.org/10.1038/s41598-022-10789-6.

[10] Vaikath, N. N., Hmila, I., Gupta, V., Erskine, D., Ingelsson, M., & El-Agnaf, O. M. A. (2019). Antibodies against alpha-synuclein: tools and therapies. *Journal of Neurochemistry*, *150*(5), 612–625. https://doi.org/10.1111/jnc.14713.

[11] Kasen, A., Houck, C., Burmeister, A. R., Sha, Q., Brundin, L., & Brundin, P. (2022). Upregulation of α-synuclein following immune activation: Possible trigger of Parkinson's disease. *Neurobiology of Disease*, *166*, 105654. https://doi.org/10.1016/j.nbd.2022.105654.

[12] Bisi, N., Feni, L., Peqini, K., Pérez-Peña, H., Ongeri, S., Pieraccini, S., & Pellegrino, S. (2021). α-Synuclein: An All-Inclusive Trip Around its Structure, Influencing Factors and Applied Techniques. *Frontiers in Chemistry*, *9*. https://doi.org/10.3389/fchem.2021.666585.

[13] Su, R., & Zhou, T. (2021). Alpha-Synuclein Induced Immune Cells Activation and Associated Therapy in Parkinson's Disease. *Frontiers in Aging Neuroscience*, *13*. https://doi.org/10.3389/fnagi.2021.769506.

[14] Tansey, M. G., & Romero-Ramos, M. (2019). Immune system responses in Parkinson's disease: Early and dynamic. *European Journal of Neuroscience*, *49*(3), 364–383. https://doi.org/10.1111/ejn.14290.

[15] Castonguay, A.-M., Gravel, C., & Lévesque, M. (2021). Treating Parkinson's Disease with Antibodies: Previous Studies and Future Directions. *Journal of Parkinson's Disease*, *11*(1), 71–92. https://doi.org/10.3233/JPD-202221.

[16] Jamal, F. (2020). Immunotherapies Targeting α - Synuclein in Parkinson Disease. *Federal Practitioner*. https://doi.org/10.12788/fp.0026.

[17] Kumar, S. T., Jagannath, S., Francois, C., Vanderstichele, H., Stoops, E., & Lashuel, H. A. (2020). How specific are the conformation-specific α-synuclein antibodies? Characterization and validation of 16 α-synuclein conformation-specific antibodies using well-characterized preparations of α-synuclein monomers, fibrils and oligomers with distinct struct. *Neurobiology of Disease*, *146*, 105086. https://doi.org/10.1016/j.nbd.2020.105086.

[18] Yan, Y., Tao, H., He, J., & Huang, S.-Y. (2020). The HDOCK server for integrated protein–protein docking. *Nature Protocols*, *15*(5), 1829–1852. https://doi.org/10.1038/s41596-020-0312-x.

[19] Ménez, R., Michel, S., Muller, B. H., Bossus, M., Ducancel, F., Jolivet-Reynaud, C., & Stura, E. A. (2008). Crystal Structure of a Ternary Complex between Human Prostate-specific Antigen, Its Substrate Acyl Intermediate and an Activating Antibody. *Journal of*

Molecular Biology, *376*(4), 1021–1033. https://doi.org/10.1016/j.jmb.2007.11.052.

[20] Rodriguez, J. A., Ivanova, M. I., Sawaya, M. R., Cascio, D., Reyes, F. E., Shi, D., … Eisenberg, D. S. (2015). Structure of the toxic core of α-synuclein from invisible crystals. *Nature*, *525*(7570), 486–490. https://doi.org/10.1038/nature15368.

[21] BIOVIA. (2016). Discovery Studio Modeling Environment,Release (2017). *San Diego: Dassault Systems*.

[22] Vidal-Limon, A., Aguilar-Toalá, J. E., & Liceaga, A. M. (2022). Integration of Molecular Docking Analysis and Molecular Dynamics Simulations for Studying Food Proteins and Bioactive Peptides. *Journal of Agricultural and Food Chemistry*, *70*(4), 934–943. https://doi.org/10.1021/acs.jafc.1c06110.

[23] Brás, I. C., & Outeiro, T. F. (2021). Alpha-Synuclein: Mechanisms of Release and Pathology Progression in Synucleinopathies. *Cells*, *10*(2), 375. https://doi.org/10.3390/cells10020375.

[24] McKay, M. J., Afrose, F., Koeppe, R. E., & Greathouse, D. V. (2018). Helix formation and stability in membranes. *Biochimica et Biophysica Acta (BBA) - Biomembranes*, *1860*(10), 2108–2117. https://doi.org/10.1016/j.bbamem.2018.02.010.

[25] Meng Zhang, H. X., Mezei, M., & Cui, M., X. Y. (2011). Molecular Docking: A Powerful Approach for Structure-Based Drug Discovery. Current Computer-Aided Drug Design. *Current Computer Aided Drug Design*, *7*(2), 146–157. https://doi.org/10.2174/157340911795677602.

[26] Ambrosetti, F., Jiménez-García, B., Roel-Touris, J., & Bonvin, A. M. J. J. (2020). Modeling Antibody-Antigen Complexes by Information-Driven Docking. *Structure*, *28*(1), 119-129.e2. https://doi.org/10.1016/j.str.2019.10.011.